

Range-Spread Target Detection in Compound Gaussian Clutter with Reciprocal of the Square Root of Gamma Texture

Yanzhao Gao^{*}, Ronghui Zhan, and Jianwei Wan

Abstract—In this paper, the range-spread target detection in compound Gaussian clutter with reciprocal of the square root of gamma (RSRG) texture is investigated. The RSRG distribution has been proved to be a good model for texture component of extremely heterogeneous radar clutter. Taking this compound Gaussian model as a spherically invariant random process (SIRP), the Neyman-Pearson optimal detector for the range-spread target detection with known target amplitude is derived firstly. By replacing the ideal target amplitude with its maximum likelihood estimate (MLE), the generalized likelihood ratio test (GLRT) is then obtained. The statistical property of the texture component is taken into account in both of these two detectors, which makes the detectors computationally complicated. A suboptimal generalized likelihood ratio test based on order statistics (OS-GLRT) is finally proposed by substituting the texture component with its MLE. The OS-GLRT makes use of some largest observations from the range cells occupied by the most likely target scatters. The performance assessment conducted by Monte Carlo simulation validates the effectiveness of the proposed detectors.

1. INTRODUCTION

The adaptive detection of point-like target against different kinds of clutter for the low-resolution radar has been studied for several decades, and some strategies were addressed partly in [1–9]. However, the application of the modern pulse compression techniques makes the high-resolution radar capable of resolving a target into a number of discrete scattering centers. These discrete scattering centers of a so-called range-spread target always occupy several range cells in the radar returns, and it could be referred to as multiple dominant scattering (MDS) centers [10]. It has been pointed out that increasing the radar range resolution can reduce the amount of energy per range cell backscattered by distributed clutter, and the radar detection performance, therefore, could be enhanced largely by making use of appropriate detection strategies [11]. However, the detection strategies for the point-like target may have poor performance for the range-spread target because they are not able to take full advantage of the backscattered energy of a target in the discrete range cells.

The detection of range-spread target embedded in different kinds of clutter background has received considerable attentions in the recent years. The detection strategies in Gaussian-distributed clutter have been investigated in [11–15]. The N out of M (N/M) detector and the integration detector are proposed in [11]. It is pointed out that the latter performs better than the former except that the target is composed of a single strong point. In [12], the optimal and suboptimal receiver frameworks are designed in the white Gaussian clutter background, which is considered as the theoretical basis of range-spread target detection. In [13], a reasonable distribution for the target scatterer density is employed in the range-spread target detection, and the scatterer density dependent generalized likelihood ratio test (SDD-GLRT) is proposed. For the singular covariance matrix, a modified generalized likelihood ratio test (MGLRT) is designed in [14]. Moreover, an orthogonal rejection MGLRT (OR-MGLRT) is introduced in [15] for range-spread target detection in correlated Gaussian noise and used as the second stage of a double threshold receiving structure.

Received 10 October 2013, Accepted 4 December 2013, Scheduled 11 December 2013

^{*} Corresponding author: Yanzhao Gao (buaagaoyz@sina.com).

The authors are with the School of Electronic Science and Engineering, National University of Defense Technology, China.

In the situations such as low grazing angles and/or high-resolution radar, the background clutter may no longer be modeled accurately as a Gaussian random variable [16]. Some heavy-tailed radar clutter models, such as K distribution [16–18], Pareto distribution [19, 20], KK distribution [21, 22], are utilized in the target detection scheme design. In [16], the K -distribution is expressed as spherically invariant random process and then two CFAR detectors, i.e., scatterer density dependent GLRT (SDD-GLRT) and non-scatterer density dependent GLRT (NSDD-GLRT), are proposed. For the case when the target scattering centers occupy only a fraction of the range cells under test, it is pointed out that the amplitudes of the so-called “hot spots” on a target are significantly greater than the other range cells. Two detectors, i.e., generalized likelihood ratio test based on order statistics (OS-GLRT) and OS-GLRT with dynamic threshold (DOS-GLRT), are discussed in [17] to overcome the “collapsing loss”. In [18], a robust detector with CFAR property is proposed, which cascades a detector based on the GLRT and two binary integrators. Validation of the resultant Pareto clutter intensity model for X-band radar returns has been included in [23, 24]. The target detectors based on Pareto distribution, i.e., the optimal detector, the GLRT detector and the whitening matched filter (WMF), are compared in [19, 20]. The optimal decision rules for the totally known constant target based on Neyman-Pearson criterion in KK -distributed radar clutter is derived in [21]. Additionally, the GLRT detector is proposed, which makes use of the MLE of the target amplitude. Both these two detectors are dependent on the modified Bessel-function of the second kind. A computationally simpler suboptimal detection scheme, using a well-known Bessel identity to eliminate the Bessel function dependence, is derived in [22]. The simulation results show that small detection losses are possible if an appropriate number of looks are chosen.

The RSRG texture model is proposed in [25] as a particular case of the square root of generalized inverse Gaussian distribution. It is capable of modeling texture component of radar clutter with different degrees of heterogeneity and has been widely applied in heavy-tailed radar clutter modeling, such as SAR clutter [26, 27], C-band scanning radar [28], etc.. In this paper, the range-spread target detection in compound Gaussian clutter with RSRG texture is investigated. The optimal detector based on Neyman-Pearson criterion with known constant target amplitude is introduced firstly. However, in a real application, the target is unknown and hence it must be estimated. By replacing the uncertain target amplitude with its MLE, the GLRT detector is then obtained. The statistical property of the texture component is considered in both of these two detectors, which makes the detectors more computationally complicated. Substituting the texture component with its MLE, the OS-GLRT is finally derived.

The remainder of this paper is organized as follows. The compound Gaussian distribution with RSRG texture is introduced in Section 2. The detection problem with target and clutter models is formulated in Section 3. Section 4 is devoted to the design of the detectors in the compound Gaussian distributed clutter, followed by their performance assessment in Section 5. The concluding remarks are given in Section 6.

2. COMPOUND GAUSSIAN MODEL WITH RSRG TEXTURE

The compound Gaussian distribution with RSRG texture is derived from the multiplicative clutter model. It takes the clutter observations as a product of two independent random variables: one (X) modeling the speckle noise and the other (Y) modeling the terrain backscatter, i.e., the texture component. Therefore, the observations are defined by the product $Z = X \cdot Y$. It is considered that both the imaginary and real part of the speckle noise can be modeled by correlated Gaussian distribution, resulting in Rayleigh distributed speckle noise, which is characterized by the density

$$f_X(x|y) = \frac{x}{y^2} \exp\left(-\frac{x^2}{2y^2}\right), \quad x, y > 0, \quad (1)$$

where y is the parameter representing the texture component.

The RSRG distribution is proposed as a special case of the square root of generalized inverse Gaussian distribution. In [25], it is pointed out that the RSRG distribution is an outstanding model for the homogeneous, heterogeneous, and extremely heterogeneous clutter data. Its probability density function (PDF) is given by

$$f_Y(y) = \frac{2}{\gamma^\alpha \Gamma(-\alpha)} y^{2\alpha-1} \exp(-\gamma/y^2), \quad -\alpha, \gamma, y > 0. \quad (2)$$

Then the compound Gaussian distribution can be written as

$$f_Z(x) = \int_0^\infty f_X(x|y)f_Y(y)dy = \frac{-\alpha x (x^2 + 2\gamma)^{\alpha-1}}{\gamma^\alpha 2^{\alpha-1}}, \quad -\alpha, \gamma, x > 0. \quad (3)$$

From (3), it can be seen that the compound Gaussian distribution is actually the single-look amplitude G^0 distribution, whose r th order moments are given by

$$E\{Z^r\} = 2^{r/2} \Gamma\left(\frac{r}{2} + 1\right) \gamma^{r/2} \frac{\Gamma(-\alpha - r/2)}{\Gamma(-\alpha)}. \quad (4)$$

3. PROBLEM FORMULATION

Assume that the radar returns are collected from N coherent pulses. The problem of range-spread target detection can be expressed as judging the presence of a range-spread target across K range cells z_k ($k = 1, 2, \dots, K$). It is supposed that the possible target is completely contained within the K range cells, and its range migration is neglected within a coherent processing interval (CPI). A secondary data set z_k ($k = K + 1, \dots, K + R$) without any useful target echo is also collected, including pure clutter with the same statistical properties as the primary data. It is also assumed that the clutter power is significantly greater than the internal noise contribution [17]. In other words, the internal noise has little effect on the detector performance. Therefore, the internal noise can be ignored, and the detection problem can be formulated in terms of the following binary hypotheses test

$$\begin{cases} H_0 : \mathbf{z}_k = \mathbf{c}_k, & k = 1, 2, \dots, K + R \\ H_1 : \begin{cases} \mathbf{z}_k = \beta_k \mathbf{p} + \mathbf{c}_k, & k = 1, 2, \dots, K \\ \mathbf{z}_k = \mathbf{c}_k, & k = K + 1, \dots, K + R \end{cases} \end{cases}, \quad (5)$$

The complex random variable β_k ($k = 1, 2, \dots, K$) accounts for target characteristics, which is assumed to be constant from scan to scan. Therefore, $|\beta_k|$ ($k = 1, 2, \dots, K$) is the target amplitude. The parameter \mathbf{p} is the steering vector, i.e., $\mathbf{p} = (1, e^{jf_0}, e^{j2f_0}, \dots, e^{j(N-1)f_0})^T$ where f_0 denotes a constant and known phase shifting, and $(\cdot)^T$ represents transpose.

The SIRP provide a general formulation of the joint density of a non-Gaussian random process. Traditionally, a SIRP is introduced as a process whose finite order subprocesses, called spherically invariant random vector (SIRV), possess a specific density. However, due to an equivalent formulation, the SIRV and SIRP can be specified in a manner more intuitive to the modeling of radar returns as follows. The N -dimension complex envelope of the clutter return \mathbf{c}_k in range cell k is called SIRV if it can be written in the compound Gaussian formulation:

$$\mathbf{c}_k = \tau_k \cdot \boldsymbol{\eta}_k, \quad k = 1, \dots, K + R, \quad (6)$$

where the texture component τ_k is a nonnegative real valued univariate random variable with density f_τ , and the speckle noise $\boldsymbol{\eta}_k = [\eta_k(1), \eta_k(2), \dots, \eta_k(N)]^T$ is zero mean complex Gaussian random vector, or multidimensional complex Gaussian process. It is assumed that τ_k and $\boldsymbol{\eta}_k$ are independent from range cell to range cell. In this paper, the texture component is modeled by RSRG distribution

$$f_\tau(\tau_k) = \frac{2}{\gamma^\alpha \Gamma(-\alpha)} \tau_k^{2\alpha-1} \exp(-\gamma/\tau_k^2), \quad -\alpha, \gamma, \tau_k > 0, \quad (7)$$

The covariance matrix $\boldsymbol{\Sigma}$ associated with $\boldsymbol{\eta}_k$ ($k = 1, 2, \dots, K + R$) is defined as

$$\boldsymbol{\Sigma} = E\{\boldsymbol{\eta}_k \boldsymbol{\eta}_k^H\}, \quad k = 1, \dots, K + R, \quad (8)$$

where $(\cdot)^H$ represents conjugate transpose.

For concise, it is assumed that in each range cell there is at most one scattering center. In many application cases, the scattering centers of a range-spread target may occupy only a fraction of the K range cells. Furthermore, the amplitudes of range cells containing target scattering centers are significantly greater than that of range cells with pure clutter [16]. If these range cells with pure clutter are integrated in the target detection process, the detection performance may be degraded, which is called ‘‘collapsing loss’’ [29]. Let Θ_J denote the index set of range cells containing target scattering

centers, where the subscript J represent the number of scattering centers, i.e., the number of effective range cells. Then the binary hypotheses test in (5) can be simplified as

$$\begin{cases} H_0 : \mathbf{z}_k = \mathbf{c}_k, & k \in \Theta_J \\ H_1 : \mathbf{z}_k = \beta_k \mathbf{p} + \mathbf{c}_k, & k \in \Theta_J \end{cases} \quad (9)$$

4. DETECTORS DESIGN

It is assumed that the normalized covariance matrix $\mathbf{\Sigma}$ in (8) and \mathbf{p} in (9) is known. According to the previous assumptions, the joint PDF of \mathbf{z}_k ($k \in \Theta_J$) conditioned on τ_k and β_k under each hypothesis is given by

$$\prod_{k \in \Theta_J} f(\mathbf{z}_k | \tau_k, \beta_k, H_i) = \prod_{k \in \Theta_J} \frac{1}{\tau_k^{2N} |\mathbf{\Sigma}|} \exp \left[-\frac{q_i(k)}{\tau_k^2} \right], \quad i = 0, 1, \quad (10)$$

where $|\cdot|$ denotes determinant, and $q_0(k) = \mathbf{z}_k^H \mathbf{\Sigma}^{-1} \mathbf{z}_k$, $q_1(k) = (\mathbf{z}_k - \beta_k \mathbf{p})^H \mathbf{\Sigma}^{-1} (\mathbf{z}_k - \beta_k \mathbf{p})$. Taking account of the RSRG distribution of the texture component τ_k , the joint conditional PDF of \mathbf{z}_k ($k \in \Theta_J$) conditioned on β_k can be expressed as

$$\begin{aligned} \prod_{k \in \Theta_J} f(\mathbf{z}_k | \beta_k, H_i) &= \prod_{k \in \Theta_J} E_{\tau} \{ f(\mathbf{z}_k | \tau_k, \beta_k, H_i) \} = \prod_{k \in \Theta_J} \int_0^{\infty} f(\mathbf{z}_k | \tau_k, \beta_k, H_i) \cdot f_{\tau}(\tau_k) d\tau_k \\ &= \prod_{k \in \Theta_J} \int_0^{\infty} \frac{1}{\tau_k^{2N} |\mathbf{\Sigma}|} \exp \left[-\frac{q_i(k)}{\tau_k^2} \right] \cdot f_{\tau}(\tau_k) d\tau_k \quad i = 0, 1. \end{aligned} \quad (11)$$

Hence if we define a function $h_S(s)$

$$h_S(s) = \int_0^{\infty} \frac{1}{\tau_k^{2N}} \exp \left[-\frac{s}{\tau_k^2} \right] \cdot f_{\tau}(\tau_k) d\tau_k \quad (12)$$

Then for the RSRG texture component, by substituting the PDF (7) in (12) it yields

$$h_S(s) = \frac{\Gamma(N - \alpha)(s + \gamma)^{\alpha - N}}{\Gamma(-\alpha)\gamma^{\alpha}} \quad (13)$$

Now the clutter joint density conditioned on β_k can be written in the compact form as

$$\prod_{k \in \Theta_J} f(\mathbf{z}_k | \beta_k, H_i) = \frac{1}{|\mathbf{\Sigma}|^J} \prod_{k \in \Theta_J} h_S(q_i(k)), \quad i = 0, 1 \quad (14)$$

The function $h_S(s)$ defined in (12) is of great importance in SIRP theory, as all densities of interest are expressed in terms of it. It is thus called the characteristic function.

4.1. The Optimal Detector

To simplify the analysis, it is assumed that the target amplitude β_k ($k \in \Theta_J$) is a fixed constant that is completely specified. The Neyman-Pearson optimal detector is the ratio of the densities under H_1 and H_0 hypothesis. Hence, according to (14), the likelihood ratio test can be expressed as

$$\lambda_{opt} = \frac{\prod_{k \in \Theta_J} h_S(q_1(k))}{\prod_{k \in \Theta_J} h_S(q_0(k))} = \frac{\prod_{k \in \Theta_J} (q_1(k) + \gamma)^{\alpha - N}}{\prod_{k \in \Theta_J} (q_0(k) + \gamma)^{\alpha - N}} \quad (15)$$

The logarithmic expression of (15) is further given by

$$\lambda_{opt} = (\alpha - N) \left(\sum_{k \in \Theta_J} \ln(q_1(k) + \gamma) - \sum_{k \in \Theta_J} \ln(q_0(k) + \gamma) \right) \quad (16)$$

Then the optimal decision rule is

$$\lambda_{opt} \underset{H_0}{\overset{H_1}{\geq}} G_{opt} \quad (17)$$

where G_{opt} is the detection threshold, which can be determined numerically from the given false alarm ratio. The notation $X \underset{H_0}{\overset{H_1}{\geq}} Y$ means that the H_0 hypothesis is rejected if and only if $X > Y$. The detection statistic in (16) is a function of the fixed target echo, which is assumed to be totally known. As a result, different thresholds G_{opt} are required to maintain a fixed false alarm ratio for varying signal to clutter ratio (SCR) and different distributions of the target energy in the J range cells.

4.2. GLRT Detector

In a real application, the amplitude of the target echo in each range cell is unknown and hence β_k ($k \in \Theta_J$) has to be estimated firstly in the target detection process. As the assumption aforementioned, the β_k ($k \in \Theta_J$) is constant from scan to scan. Then these parameters are estimated by the ML estimator. By applying the MLE to (17), the GLRT detector with known covariance matrix Σ can be derived as

$$\lambda_{GLRT} = \frac{\max_{\beta_k} \prod_{k \in \Theta_J} h_S(q_1(k))}{\prod_{k \in \Theta_J} h_S(q_0(k))} \underset{H_0}{\overset{H_1}{\geq}} G_{GLRT} \quad (18)$$

where G_{GLRT} is the detection threshold. The MLE of β_k ($k \in \Theta_J$) can be obtained by maximizing the function $h_N(q_1(k))$ in (14), i.e.,

$$\hat{\beta}_k = \frac{\mathbf{p}^H \Sigma^{-1} \mathbf{z}_k}{\mathbf{p}^H \Sigma^{-1} \mathbf{p}}, \quad k \in \Theta_J \quad (19)$$

From (19) and (18), the logarithmic expression of GLRT detector is given by

$$\lambda_{GLRT} = (\alpha - N) \left(\sum_{k \in \Theta_J} \ln(\hat{q}_1(k) + \gamma) - \sum_{k \in \Theta_J} \ln(q_0(k) + \gamma) \right) \underset{H_0}{\overset{H_1}{\geq}} G_{GLRT} \quad (20)$$

where $\hat{q}_1(k)$ denotes the estimate of $q_1(k)$ with $\hat{\beta}_k$ in (19).

4.3. OS-GLRT Detector

Both of the statistical properties of the two components, i.e., the speckle noise and texture component are considered in the optimal detector and the GLRT detector. Considering that 1) the number and the location of the range cells containing target scattering centers are unknown, i.e., the set Θ_J is unknown; 2) it is computationally complicated to obtain the MLE of β_k ($k \in \Theta_J$), the aforementioned two detectors are not practicable in the real scenarios. In this subsection, the GLRT detector based on order statistics is proposed, in which the statistical property of the texture component is ignored, and the true τ_k ($k \in \Theta_J$) in the range cells are replaced by their MLEs. According to the OS method, some largest observations from the range cells occupied by the most likely target scattering centers are utilized to overcome the “collapsing loss” resulting from the lack of scattering center information.

Under the assumption that the normalized clutter covariance matrix Σ is known, the GLRT without the statistical property of texture component can be derived from

$$\lambda_{GLRT} = \frac{\max_{\tau} \max_{\beta} \prod_{k \in \Theta_J} f(\mathbf{z}_k | \tau_k, \beta_k, H_1)}{\max_{\tau} \prod_{k \in \Theta_J} f(\mathbf{z}_k | \tau_k, H_0)} \underset{H_0}{\overset{H_1}{\geq}} G_{GLRT} \quad (21)$$

By substituting (10) in (21), the GLRT can be written as

$$\lambda_{\text{GLRT}} = \frac{\max_{\tau} \max_{\beta} \prod_{k \in \Theta_J} \frac{1}{\tau_k^{2N}} \exp \left[-\frac{q_1(k)}{\tau_k^2} \right]}{\max_{\tau} \prod_{k \in \Theta_J} \frac{1}{\tau_k^{2N}} \exp \left[-\frac{q_0(k)}{\tau_k^2} \right]} \quad (22)$$

In (22), the MLE of τ_k ($k \in \Theta_J$) under the hypotheses H_0 and H_1 can be derived by utilizing the MLE of β_k ($k \in \Theta_J$) in (19) as

$$\begin{aligned} H_0 : \hat{\tau}_k &= \frac{1}{2N} \hat{q}_0(k) \\ H_1 : \hat{\tau}_k &= \frac{1}{2N} \hat{q}_1(k) \end{aligned} \quad (23)$$

Substituting (19) and (23) into (22), the GLRT is denoted as

$$\lambda_{\text{GLRT}} = -2(N-1) \sum_{k \in \Theta_J} \ln \left[1 - \frac{|\mathbf{p}^H \boldsymbol{\Sigma}^{-1} \mathbf{z}_k|^2}{(\mathbf{z}_k^H \boldsymbol{\Sigma}^{-1} \mathbf{z}_k) (\mathbf{p}_k^H \boldsymbol{\Sigma}^{-1} \mathbf{p}_k)} \right] \underset{H_0}{\overset{H_1}{\gtrless}} G_{\text{GLRT}} \quad (24)$$

Define a quantity w_k as

$$w_k = \frac{|\mathbf{p}^H \boldsymbol{\Sigma}^{-1} \mathbf{z}_k|^2}{(\mathbf{z}_k^H \boldsymbol{\Sigma}^{-1} \mathbf{z}_k) (\mathbf{p}_k^H \boldsymbol{\Sigma}^{-1} \mathbf{p}_k)}, \quad (25)$$

which is part of the detection statistical in (24). From the previous formula, the quantity w_k can be interpreted as the normalized energy of \mathbf{z}_k after matched filtering. Then the set Θ_J can be estimated according to the values of normalized energy w_k [17]. In sort descending, the order statistics of w_k ($k \in \Theta_K$) are denoted as

$$w_{(1)} \geq w_{(2)} \geq \dots \geq w_{(k)} \geq \dots \geq w_{(K)} \quad (26)$$

Hence, the detection statistic of the OS-GLRT detector can be obtained from the first J elements of the set $w_{(k)}$ ($k = 1, 2, \dots, J$) as

$$\lambda_{\text{OS-GLRT}} = -2(N-1) \sum_{k=1}^J \ln (1 - w_{(k)}) \underset{H_0}{\overset{H_1}{\gtrless}} G_{\text{OS-GLRT}} \quad (27)$$

where $G_{\text{OS-GLRT}}$ is the detection threshold of the OS-GLRT detector.

5. PERFORMANCE ASSESSMENT

The performance of the optimal detector, GLRT detector, and OS-GLRT detector are assessed by the Monte-Carlo simulation in this section. It is assumed that the normalized covariance matrix $\boldsymbol{\Sigma}$ is Toeplitz, and the power spectrum density (PSD) of the speckle noise is supposed to be Lorentzian. Therefore, the clutter samples are generated from an exponential correlation structure, i.e., the elements of the matrix $\boldsymbol{\Sigma}$ is given by [30]

$$[\boldsymbol{\Sigma}]_{i,j} = \gamma_c^{|i-j|}, \quad 1 \leq i, j \leq N \quad (28)$$

where the parameter γ_c denotes the one-lag correlation coefficient.

The texture is modeled by the RSRG distribution as given in (7), in which α is the shape parameter controlling the deviation from Gaussian statistics and γ is the scale parameter indicating the mean of the distribution. Without loss of generality, the scale parameter γ is set as $\gamma = 10$. Firstly, a group of clutter samples with RSRG texture are generated for the shape parameter $\alpha = -1.5$. The amplitudes of the target scattering centers in the range cells are assumed to be independent identical distribution (IID), zero-mean complex circular Gaussian random vectors (RV) with the variance $E\{|\beta_k|^2\} = \varepsilon_k \sigma_s^2 K$ ($k \in \Theta_J$), where ε_k implies the fraction of the total energy in the given range cell

Table 1. Values of ε_k for typical MDS models.

Model	Range Cell Number			
Number	1	2	...	J
1	$1/J$	$1/J$	$1/J$	$1/J$
2	0.5	$0.5/(J-1)$	$0.5/(J-1)$	$0.5/(J-1)$
3	0.9	$0.1/(J-1)$	$0.1/(J-1)$	$0.1/(J-1)$

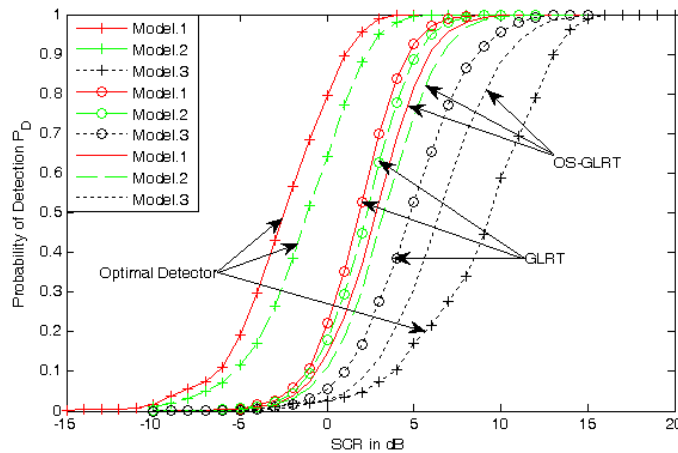
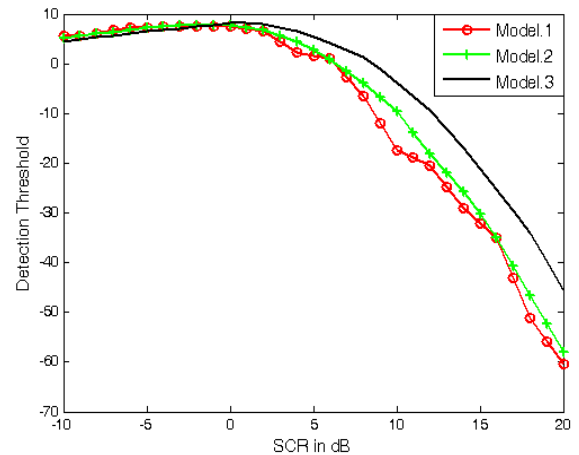
k , and the σ_s^2 indicates the average signal power per range cell. In this paper, three typical multiple dominant scatters models are considered in Table 1.

The performance of these detectors depend on the parameters, such as $\beta_k (k \in \Theta_J)$, \mathbf{p} , etc., only through the input SCR defined as

$$\text{SCR} = \frac{\sigma_s^2}{\sigma_c^2} \mathbf{p}^H \Sigma^{-1} \mathbf{p} \quad (29)$$

where $\sigma_c^2 = E(|\mathbf{c}|^2) = 2\gamma/(-\alpha - 1)$ indicates the average clutter power per range cell. It is really hard to compute the analytic detection threshold for a given false alarm probability P_F . Alternatively, the thresholds are obtained by Monte-Carlo simulation. Moreover, the probability of detection P_D is estimated based on Monte-Carlo simulation. The trials of Monte-Carlo simulations used to calculate P_F and P_D are $100/P_F$ and 10000, respectively. In order to alleviate the computational burden, it is assumed that $P_F = 10^{-4}$, and the other parameters are set to be $K = 12$, $J = 5$, $N = 5$, $f_0 = 0.4$, $\gamma_c = 0.99$.

Firstly, the effect of different MDS models on the performance of these three detectors is evaluated. In Figure 1, the plots of P_D versus SCR of the three detectors are given for the three different MDS models in Table 1. It can be seen from the plots that all the three detectors has the best performance with MDS Model 1, where the target energy is uniformly distributed in J range cells. If most of the target energy is concentrated in one range cell, the performance of the three detectors is degraded. From (16), (20), and (27), the detection statistics of the three detectors are expressed as the product or logarithmic sum of the returns in the J range cells. Therefore, if the total target energy in all the J range cells is given, it can be concluded that the detection statistics achieve their maximum value when the target energy is uniformly distributed. Contrarily, if the target energy is gradually concentrated, the three detection statistics are all getting smaller, which results in significant detection loss.

**Figure 1.** P_D versus SCR of the three detectors with MDS Model 1–Model 3.**Figure 2.** Detection threshold of the optimal detector versus SCR with the MDS Model 1–Model 3.

If the target energy is uniformly distributed, taking the MDS Model 1 as an example, it can be seen that the optimal detector has the best performance, and the performance of OS-GLRT detector is the most poor. It also can be seen that the optimal detector is much better than the GLRT detector; and the performance discrepancy of the OS-GLRT detector and GLRT detector is not that evident. This means that the primary factor which affects the detector performance mostly is the estimation accuracy of the amplitude $\beta_k (k \in \Theta_J)$; and the statistical property of the texture has much less influence. If the target energy is concentrated, taking the MDS Model 3 for example, the GLRT detector has the best performance and the performance of the optimal detector, contrarily, is very poor. This means that the optimal detector is significantly affected by different MDS models.

The detection statistic of the optimal detector is obtained under the condition that the target amplitudes are totally known. As aforementioned, the detection threshold must be changed to maintain a fixed P_F for different SCRs or/and different distributions of the target energy in the J range cells. In Figure 2, the detection threshold of the optimal detector versus SCR is plotted for the three MDS models. It is seen from Figure 2 that the detection thresholds for the three MDS models have the same trend, and all of them are not monotone with the SCR increasing from -10 dB to 20 dB. For the range cells without target scattering centers, since 1) the variable q_1 is increasing when the SCR is below 0 dB, and it is degressive if the SCR is greater than 0 dB; 2) the detection statistic of the optimal detector in (16) is a monotonically increasing function of q_1 , the detection statistic increases firstly and then decreases as the same as q_1 . As a result, the detection thresholds changes as in Figure 2 to maintain a fixed P_F .

Table 2 lists the runtimes of the three detectors for 10000 Monte-Carlo trials. From this table, the runtime consumed by the OS-GLRT detector is roughly as long as the optimal detector. The GLRT detector, however, consumes much more runtime because the amplitudes of the target scattering centers must be estimated in its procedure. Considering that: 1) the target energy is always totally unknown in the real applications; 2) the GLRT is computationally expensive, the OS-GLRT detector, therefore, is more applicable in the compound Gaussian clutter with RSRG texture.

Table 2. The runtimes of the three detectors for 10000 Monte-Carlo trials.

Detectors	Optimal Detector	GLRT Detector	OS-GLRT Detector
Runtime/s	8.2325	12.7317	8.2183

Then the performance of the OS-GLRT detector with different parameters is considered. The performance of the OS-GLRT detector is compared for different false alarm rate, i.e., $P_F = 10^{-6}$ and $P_F = 10^{-4}$, in Figure 3. It can be seen clearly that the P_D declines when the P_F decrease from 10^{-4} to 10^{-6} for all the three models. For the Model 3, the variation of the probability P_D is up to 0.3702 ,

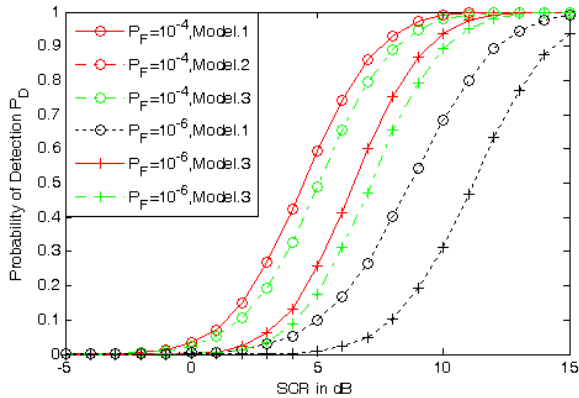


Figure 3. P_D versus SCR of the OS-GLRT detector for different P_F .

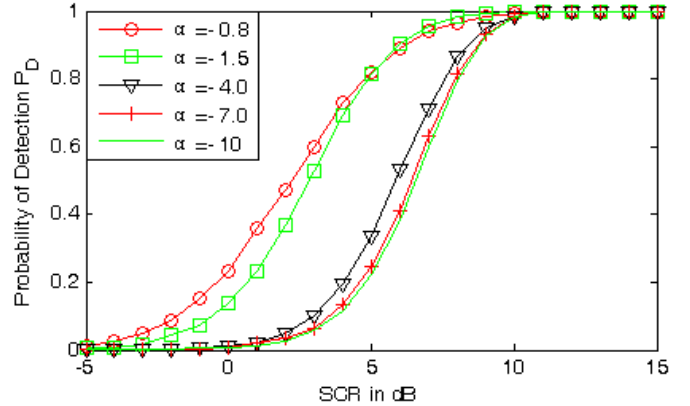


Figure 4. P_D versus SCR of the OS-GLRT detector with different shape parameter α .

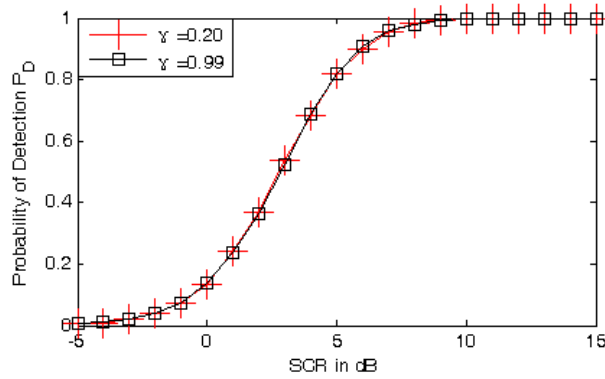


Figure 5. P_D versus SCR of the OS-GLRT detector with different one-lag correlation coefficient γ_c .

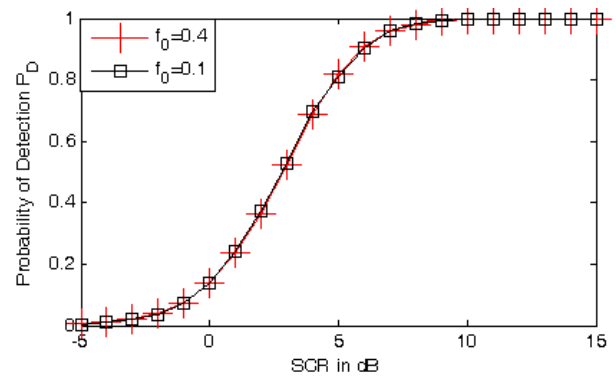


Figure 6. P_D versus SCR of the OS-GLRT detector with different constant phase shifting f_0 .

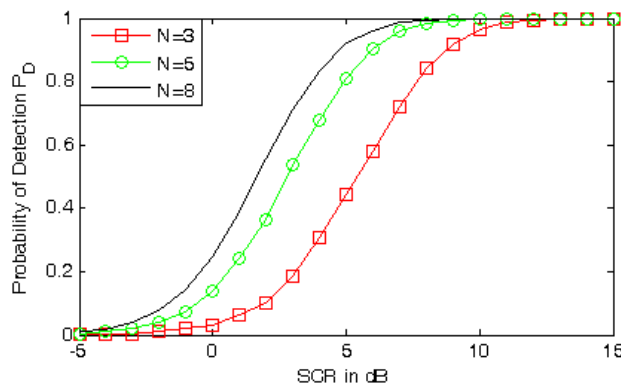


Figure 7. P_D versus SCR of the OS-GLRT detector with different N .

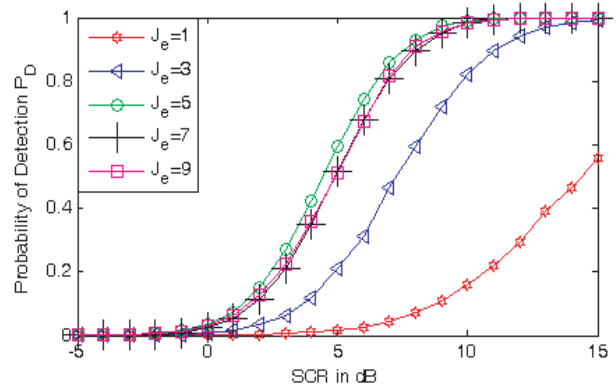


Figure 8. P_D versus SCR of the OS-GLRT detector with different estimated number of scattering centers J_e .

which is much greater than the ones for the Model 1. It means that the effect of P_F on the probability of detection is more evidently if the target energy is more un-uniformly distributed.

Figure 4 plots the probability of detection versus SCR of the OS-GLRT detector with different shape parameter α of the RSRG texture. The results indicate that the detection performance is improved evidently as the shape parameter α increases from -10 to -0.8 . According to [25], the shape parameter α is related to the degree of homogeneity. Concretely, a larger α suggests more heterogeneous clutter region. Therefore, the OS-GLRT performs better in the target detection against more heterogeneous clutter. The performance of the OS-GLRT detector with different one-lag correlation coefficient γ_c and constant phase shifting f_0 is given in Figure 5 and Figure 6. The figures show that the OS-GLRT detector is not affected by these two parameters. In Figure 7, the curves of P_D versus SCR for OS-GLRT detector are given with different numbers of coherent pulse N . It is observed that the detection performance is improved evidently as N increases from 3 to 8.

Let J_e denotes the estimated number of the scattering centers. All the simulation results in Figure 3–Figure 7 of the OS-GLRT detector are obtained for the match case, i.e., the estimated number of scattering centers equals the actual one ($J_e = J$). However, the actual number of scattering centers of a range-spread target is always unknown and cannot be estimated exactly in the real application. The P_D versus SCR of the OS-GLRT detector for different J_e are plotted in Figure 8 for $J = 5$. It is observed that the OS-GLRT detector performs best in the match case. When the estimated number of scattering centers is larger than the actual one ($J_e = 7, 9$), the SCR loss due to mismatch is small; however, when the estimated number of scattering centers is smaller than the actual one ($J_e = 1, 3$), OS-GLRT is

degraded sharply, especially for $J_e = 1$. The reason account for this is that some of the range cells occupied by target scattering centers are not integrated in the statistic detection for OS-GLRT when $J_e < J$.

6. CONCLUSIONS

In this paper, the range-spread target detection in the compound Gaussian distributed clutter with RSRG texture is studied. Three detectors, i.e., the optimal detector, GLRT detector, and the OS-GLRT detector, are considered. Base on the simulation results, it can be concluded that:

- 1) The optimal detector has the best performance if the target energy is uniformly distributed. However, it has a severely detection loss if most of the target energy is concentrated in one range cell.
- 2) The detection threshold of the optimal detector must be changed to maintain a constant false alarm probability for different SCRs or/and distributions of target energy.
- 3) The GLRT is computationally expensive compared with the other two detectors because of the estimation of the target energy in its procedure.
- 4) The OS-GLRT detector is carried out without the statistical property of the texture. It has worse performance than the others if the target energy is uniformly distributed. However, it is computationally cheaper than the others. Moreover, it performs very well if the target energy is concentrated.
- 5) The OS-GLRT detector is hardly affected by the one-lag correlation coefficient γ_c and the constant phase shifting f_0 . It is more applicable for the range-spread target detection in the compound Gaussian distributed clutter with RSRG texture, especially in the heterogeneous region.
- 6) The OS-GLRT detector is more robust for the case when the estimated number of scattering centers is larger than the actual ($J_e > J$) than the cases when $J_e < J$.

ACKNOWLEDGMENT

This work was supported in part by National Science Foundation of China (Grant No. 61002022).

REFERENCES

1. Kelly, E. J., "An adaptive detection algorithm," *IEEE Transactions on Aerospace and Electronic Systems*, Vol. 22, No. 1, 115–127, 1986.
2. Robey, F. C., et al., "A CFAR adaptive matched filter detector," *IEEE Transactions on Aerospace and Electronic Systems*, Vol. 28, No. 1, 208–216, 1992.
3. Hansen, V. G., "Constant false alarm rate processing in search radars," *Proceedings of the IEEE 1973 International Radar Conference*, 325–332, London, 1973.
4. Zhou, W., J. T. Wang, H. W. Chen, and X. Li, "Signal model and moving target detection based on MIMO synthetic aperture radar," *Progress In Electromagnetics Research*, Vol. 131, 311–329, 2012.
5. Hao, C., F. Bandiera, J. Yang, D. Orlando, S. Yan, and C. Hou, "Adaptive detection of multiple point-like targets under conic constraints," *Progress In Electromagnetics Research*, Vol. 129, 231–250, 2012.
6. Hatam, M., A. Sheikhi, and M. A. Masnadi-Shirazi, "Target detection in pulse-train MIMO radars applying ICA algorithms," *Progress In Electromagnetics Research*, Vol. 122, 413–435, 2012.
7. Tian, B., D. Y. Zhu, and Z. D. Zhu, "A novel moving target detection approach for dual-channel SAR system," *Progress In Electromagnetics Research*, Vol. 115, 191–206, 2011.
8. Gao, F., A. Ru, J. Sun, and A. Hussain, "A novel SAR target detection algorithm based on contextual knowledge," *Progress In Electromagnetics Research*, Vol. 142, 123–140, 2013.
9. Mohammadpoor, M., R. S. A. Raja Abdullah, A. Ismail, and A. F. Abas, "A circular synthetic aperture radar for on-the-ground object detection," *Progress In Electromagnetics Research*, Vol. 122, 269–292, 2012.
10. Wehner, D. R., *High-resolution Radar*, Artech House, Norwood, MA, 1995.

11. Hughes, P. K., "A high-resolution radar detection strategy," *IEEE Transactions on Aerospace and Electronic Systems*, Vol. 19, No. 5, 663–667, 1983.
12. Van Trees, H. L., *Detection Estimation and Modulation Theory*, Wiley, New York, 1971.
13. Gerlach, K., M. Steiner, and F. C. Lin, "Detection of a spatially distributed target in white noise," *IEEE Signal Processing Letters*, Vol. 4, No. 7, 198–200, 1997.
14. Maio, A. D., A. Farina, and K. Gerlach, "Adaptive detection of range spread targets with orthogonal rejection," *IEEE Transactions on Aerospace and Electronic Systems*, Vol. 43, No. 2, 738–752, 2007.
15. Gerlach, K. and M. J. Steiner, "Adaptive detection of range distributed targets," *IEEE Transactions on Signal Processing*, Vol. 47, No. 7, 1844–1851, 1999.
16. Gerlach, K., "Spatially distributed target detection in non-Gaussian clutter," *IEEE Transactions on Aerospace and Electronic Systems*, Vol. 35, No. 3, 926–934, 1999.
17. He, Y., T. Jian, et al., "Novel range-spread target detectors in non-Gaussian clutter," *IEEE Transactions on Aerospace and Electronic Systems*, Vol. 46, No. 3, 1312–1328, 2010.
18. Jian, T., Y. He, F. Su, et al., "Cascaded detector for range-spread target in non-Gaussian clutter," *IEEE Transactions on Aerospace and Electronic Systems*, Vol. 48, No. 2, 1713–1725, 2012.
19. Weinberg, G. V., "Coherent multi-look radar detection for targets in Pareto distributed clutter," Defence Science and Technology Organization, 2012.
20. Weinberg, G. V., "Coherent CFAR detection in compound Gaussian clutter with inverse gamma texture," *EURASIP Journal on Advances in Signal Processing*, Vol. 2013, 105, 2013.
21. Weinberg, G. V., "Coherent multi-look radar detection for targets in KK -distributed clutter," *Digital Communication*, 2012.
22. Weinberg, G. V., "Suboptimal coherent radar detection in a KK -distributed clutter environment," *International Scholarly Research Network Signal Processing*, 2012.
23. Balleri, A., A. Nehorai, and J. Wang, "Maximum likelihood estimation for compound-Gaussian clutter with inverse-gamma texture," *IEEE Transactions on Aerospace and Electronic Systems*, Vol. 43, No. 2, 775–780, 2007.
24. Weinberg, G. V., "Assessing the Pareto fit to high resolution high grazing angle sea clutter," *Electronics Letters*, Vol. 47, No. 8, 516–517, 2011.
25. Frery, A. C., H. J. Müller, C. F. Yanasse, et al., "A model for extremely heterogeneous clutter," *IEEE Transactions on Geoscience and Remote Sensing*, Vol. 35, No. 3, 648–659, 1997.
26. Moser, G., J. Zerubia, and S. B. Serpico, "Dictionary-based stochastic expectation-maximization for SAR amplitude probability density function estimation," *IEEE Transactions on Geoscience and Remote Sensing*, Vol. 44, No. 1, 188–200, 2006.
27. Moser, G., J. Zerubia, and S. B. Serpico, "SAR amplitude probability density function estimation based on a generalized Gaussian model," *IEEE Transactions on Image Processing*, Vol. 15, No. 6, 1429–1442, 2006.
28. Xu, Z., "Modeling of sea clutter and target detection in sea clutter," Graduate School of National University of Defense Technology, Changsha, China, 2012.
29. Nitzberg, R., "Effect of a few dominant specular reflectors target model upon target detection," *IEEE Transactions on Aerospace and Electronic Systems*, Vol. 14, No. 4, 670–673, 1978.
30. Gini, F. and M. Greco, "Covariance matrix estimation for CFAR detection in correlated heavy tailed clutter," *Signal Processing*, Vol. 82, 1495–1507, 2002.